Testing Atmospheric Oxidation in an Alabama Forest

PHILIP A. FEINER,[a] WILLIAM H. BRUNE,[a] DAVID O. MILLER,[a] LI ZHANG,[a] RONALD C. COHEN,[b] PAUL S. ROMER,[b] ALLEN H. GOLDSTEIN,[b] FRANK N. KEUTSCH,[c,d] KATE M. SKOG,[d] PAUL O. WENNBERG,[e] TRAN B. NGUYEN,[e] ALEX P. TENG,[e] JOOST DEGOUW,[f,g] ABIGAIL KOSS,[f,g] ROBERT J. WILD,[g] STEVEN S. BROWN,[g] ALEX GUENTHER,[h] ERIC EDGERTON,[i] KARSTEN BAUMANN,[i] AND JULIANE L. FRY[j]

[a] *Department of Meteorology and Atmospheric Science, The Pennsylvania State University, University Park, Pennsylvania*
[b] *University of California, Berkeley, Berkeley, California*
[c] *John A. Paulson School of Engineering and Applied Sciences, and Department of Chemistry and Chemical Biology, Harvard University, Cambridge, Massachusetts*
[d] *Department of Chemistry, University of Wisconsin–Madison, Madison, Wisconsin*
[e] *California Institute of Technology, Pasadena, California*
[f] *Cooperative Institute for Research in Environmental Sciences, University of Colorado Boulder, Boulder, Colorado*
[g] *National Oceanic and Atmospheric Administration/Earth System Research Laboratory, Boulder, Colorado*
[h] *Department of Earth System Science, University of California, Irvine, Irvine, California*
[i] *Atmospheric Research and Analysis, Inc., Cary, North Carolina*
[j] *Department of Chemistry, Reed College, Portland, Oregon*

(Manuscript received 9 February 2016, in final form 16 August 2016)

ABSTRACT

The chemical species emitted by forests create complex atmospheric oxidation chemistry and influence global atmospheric oxidation capacity and climate. The Southern Oxidant and Aerosol Study (SOAS) provided an opportunity to test the oxidation chemistry in a forest where isoprene is the dominant biogenic volatile organic compound. Hydroxyl (OH) and hydroperoxyl (HO_2) radicals were two of the hundreds of atmospheric chemical species measured, as was OH reactivity (the inverse of the OH lifetime). OH was measured by laser-induced fluorescence (LIF) and by taking the difference in signals without and with an OH scavenger that was added just outside the instrument's pinhole inlet. To test whether the chemistry at SOAS can be simulated by current model mechanisms, OH and HO_2 were evaluated with a box model using two chemical mechanisms: Master Chemical Mechanism, version 3.2 (MCMv3.2), augmented with explicit isoprene chemistry and MCMv3.3.1. Measured and modeled OH peak at about 10^6 cm^{-3} and agree well within combined uncertainties. Measured and modeled HO_2 peak at about 27 pptv and also agree well within combined uncertainties. Median OH reactivity cycled between about 11 s^{-1} at dawn and about 26 s^{-1} during midafternoon. A good test of the oxidation chemistry is the balance between OH production and loss rates using measurements; this balance was observed to within uncertainties. These SOAS results provide strong evidence that the current isoprene mechanisms are consistent with measured OH and HO_2 and, thus, capture significant aspects of the atmospheric oxidation chemistry in this isoprene-rich forest.

1. Introduction

Copious emissions of biogenic volatile organic compounds (BVOCs) dictate the atmospheric chemical composition and chemistry in forests. During the day, these BVOCs are oxidized primarily through reactions with the hydroxyl radical (OH) and ozone (O_3), which leads to the production of many oxygen-containing volatile, semivolatile, and low-volatility compounds and secondary organic aerosol. Because forests blanket almost a third of the global land, understanding forest

Denotes Open Access content.

Supplemental information related to this paper is available at the Journals Online website: http://dx.doi.org/10.1175/JAS-D-16-0044.s1.

Corresponding author address: William H. Brune, Department of Meteorology and Atmospheric Science, The Pennsylvania State University, 503 Walker Building, University Park, PA 16802.
E-mail: whb2@psu.edu

DOI: 10.1175/JAS-D-16-0044.1

oxidation chemistry is an important part of understanding atmospheric chemistry on a global scale.

OH is the main oxidative agent in the atmosphere owing to its high production rate and high reactivity (Levy 1971). In addition, the closely related hydroperoxyl radical (HO_2) is a critical reactant in oxidation pathways and often a major source of OH (Monks 2005). The cycling between OH and HO_2, collectively referred to as HO_x, is rapid. Thus, it is important to understand the behavior of both OH and HO_2.

Several field campaigns have included measurements of HO_x. Measured HO_x is then typically compared with results from photochemical box models that are constrained by other simultaneous measurements. Agreement between HO_x measurements and photochemical box model results to within uncertainties indicates that the models are correctly simulating the HO_x chemistry in these environments, especially when these comparisons are checked as a function of key variables such as temperature, sunlight, and the abundances of other chemical species.

For many regions in the atmosphere, measured and modeled OH often agree to within uncertainties. These regions include the free troposphere, the lower stratosphere, and even some polluted urban areas (Wennberg et al. 1994; Cantrell et al. 2003; Ren et al. 2008, 2012; Stone et al. 2012 and references therein; Rohrer et al. 2014). Forests are a different matter; there are few forest measurements for which OH measurements are in general agreement with properly constrained models (McKeen et al. 1997; Ren et al. 2006; Kim et al. 2013). In many forest studies, measured OH has greatly exceeded model calculation, with discrepancies of up to a factor of 10 in some cases (Tan et al. 2001; Carslaw et al. 2001; Ren et al. 2008; Lelieveld et al. 2008; Kubistin et al. 2010; Martinez et al. 2010; Hofzumahaus et al. 2009; Lou et al. 2010; Pugh et al. 2010; Stone et al. 2011; Wolfe et al. 2011; Whalley et al. 2011; Taraborrelli et al. 2012).

Forests emit abundant biogenic VOCs (BVOCs) that react rapidly with OH. Besides having high levels of BVOCs, forests often have low levels of nitrogen oxides (NO_x), which affect the pathways in the oxidation chemistry. Because OH production and loss are in balance due to the short OH lifetime, the OH concentration is proportional to the production rate (molecules per cubic centimeter per second) divided by the loss frequency (s^{-1}). The loss frequency that is calculated from models or from measurements of other chemical species is typically less than measured (Di Carlo et al. 2004; Nölscher et al. 2012). So, for measured OH to be greater than modeled OH, there must be unknown OH sources, which could be either primary sources, such as photolysis of an unknown chemical species, or secondary sources, such as recycling of HO_x to OH within the BVOC oxidation mechanisms.

These discrepancies and the speculation about OH recycling have led to increased interest in the detailed chemical oxidation mechanisms for these BVOCs, particularly isoprene (Paulot et al. 2009; Peeters et al. 2009; Peeters and Müller 2010; Crounse et al. 2011, 2012, 2013; Praske et al. 2015; St. Clair et al. 2015). Initially one isomerization mechanism showed promise to resolve this discrepancy for isoprene-dominated forests by rapidly producing OH (Peeters et al. 2009, Peeters and Müller 2010; Taraborrelli et al. 2012), but subsequent laboratory and theoretical work has demonstrated that this mechanism, while it does occur, is not fast enough to explain the high OH measurements (Crounse et al. 2011; Peeters et al. 2014). On the other hand, a recent laboratory study provides evidence for OH regeneration during isoprene oxidation (Fuchs et al. 2013). Thus, while progress has been made in understanding the isoprene oxidation mechanism, the issue of the amount of OH regeneration is not yet completely resolved.

An alternative explanation for the high OH concentrations observed in forests is that some previous OH field measurements are wrong. In 2009, to explore the possibility that the Penn State OH laser-induced fluorescence (LIF) measurement suffered from an interference, a second method of OH measurement was implemented involving the chemical scavenging of ambient OH to separate the ambient OH signal from the background LIF signal. This method was used along with the typical LIF technique of tuning the laser to a wavelength at which OH absorbs and fluoresces and then to a nearby wavelength to get the background—a sequence called wavelength modulation.

The first forest measurements using both techniques were made with the Penn State OH LIF instrument during the Biosphere Effects of Aerosols and Photochemistry Experiment (BEARPEX) in a California Sierra Nevada forest (Mao et al. 2012). This forest's chemistry is dominated by 2-methyl–3-buten–2-ol (MBO), terpenes, and, in the late afternoon, isoprene products. This study showed that the chemical scavenging technique removed the abundant OH generated by the photolysis of water vapor with a UV lamp, thus proving that chemical scavenging can successfully remove OH in the atmosphere. The OH measured with chemical scavenging matched OH from models that had updated chemical mechanisms and was 2–3 times smaller than the OH values determined by the widely used wavelength modulation technique. We determined that, in our instrument, the wavelength modulation method suffers from an interference and that the chemical scavenging method measures ambient OH.

Shortly thereafter, OH measurements using LIF and chemical scavenging were directly compared to measurements by another technique, selective ionization chemical mass spectrometery (SICIMS), during the Hyytiälä United Measurements of Photochemistry and Particles in Air–Comprehensive Organic Precursor Emission and Concentration study (HUMPPA-COPEC-2010). This study took place in a southern Finland forest where a mixture of terpenes dominates the atmospheric chemistry. Measurements taken during HUMPPA-COPEC-2010 with the Mainz LIF instrument using the chemical scavenging technique agreed with the SICIMS technique to within uncertainties (Hens et al. 2014). Both OH measurements agreed with OH calculated with a photochemical box model. This result from an instrument that is similar to ours lends further credence to the hypothesis that the OH discrepancy reported previously using our instrument was due to an interference affecting our LIF measurements using wavelength modulation.

The Southern Oxidant and Aerosol Study (SOAS) occurred during summer 2013 in a southeastern U.S. forest where isoprene is the dominant BVOC emission. This study deployed one of the most comprehensive chemical measurement suites ever assembled for atmospheric chemistry (Carlton et al. 2016, manuscript submitted to *Bull. Amer. Meteor. Soc.*). Data from SOAS provided a highly constrained test of HO_x chemistry using OH measurements free from interference. In addition, the extensive chemical measurement suite enabled a thorough test of many different aspects of the atmospheric oxidation there, including HO_2 and OH reactivity.

2. Methods

a. Measurement site

SOAS was a part of the larger Southern Atmosphere Study (SAS) that was focused on forest emissions of BVOCs, forest oxidation chemistry, secondary organic aerosol (SOA) formation and aging, and deposition of gases and particles. A more comprehensive understanding of these processes has widespread applications, from improving the quality of regional pollution models to better predicting climate change (Carlton et al. 2016, manuscript submitted to *Bull. Amer. Meteor. Soc.*).

SOAS data were collected at several locations and on several platforms from 5 June to 16 July 2013. The main SOAS site was near Brent, Alabama, just within the Talladega National Forest (32.902 89°N, 87.249 68°W) at the Centerville (CTR) SouthEastern Aerosol Research and Characterization (SEARCH) Network monitoring site (Hansen et al. 2003). The site was in a small clearing surrounded on all sides by a dense mixed forest composed of pine and broadleaf species such as oak. The canopy height of the forest at the site was between 9 and 12 m. This forest emitted mainly isoprene but also smaller abundances of other BVOCs such as α-pinene. The site is relatively isolated from intense anthropogenic sources but did experience occasional influence from Birmingham (70 km to the northeast), Tuscaloosa (50 km to the northwest), natural gas power plants (>50 km to the southeast), and traffic on local roads.

The Brent site had measurements situated in two main areas. The first area featured a group of trailers where most aerosol properties were measured. About 100 m away and slightly downhill from the main area, two trailers and an 18-m-tall scaffolding tower were sited in a small clearing closely surrounded by the forest on three sides. The top of the tower housed inlets for several gas-phase and meteorological instruments and three large instruments, including the instrument to measure HO_x that is discussed in this paper.

b. HO_x measurements

HO_x measurements at the SOAS site were made with Penn State's Ground-based Tropospheric Hydrogen-Oxides Sensor (GTHOS) (Faloona et al. 2004), which measures OH by LIF (Fig. 1). OH is sampled through a 1-mm aperture and is pulled through the detection axes at low pressure (~6 hPa). The air sample passes through the path of a laser tuned to the $Q_1(2)$ OH absorption line (~308 nm). Fluorescence from OH is detected by a gated microchannel plate detector. Downstream of the OH measurement region, HO_2 is measured by adding reagent NO to the airflow, which converts HO_2 to OH, and this OH is detected by LIF in a second detection axis. The 308-nm light is produced by an Nd:YAG-pumped tunable dye laser and is tuned to the wavelength of an OH absorption line and then to a wavelength off the line, alternating in successive 30-s cycles between a wavelength either greater or less than the absorption line wavelength. The difference between the two signals is proportional to OH in the instrument. The proportionality constant is determined by laboratory and field calibrations (Faloona et al. 2004). This method of measuring OH, referred to as OH_{wave}, has been used in nearly all previous LIF measurements of OH.

The second measurement method involves injecting a chemical, hexafluoropropylene (C_3F_6), into the ambient air to scavenge the OH before it is sampled through the instrument inlet (Fig. 1). The amount of reactant is chosen to maximize the fraction of OH removed in the ~10 ms that the air takes to travel between scavenger injection and entering the instrument inlet and to simultaneously minimize the OH removed inside the

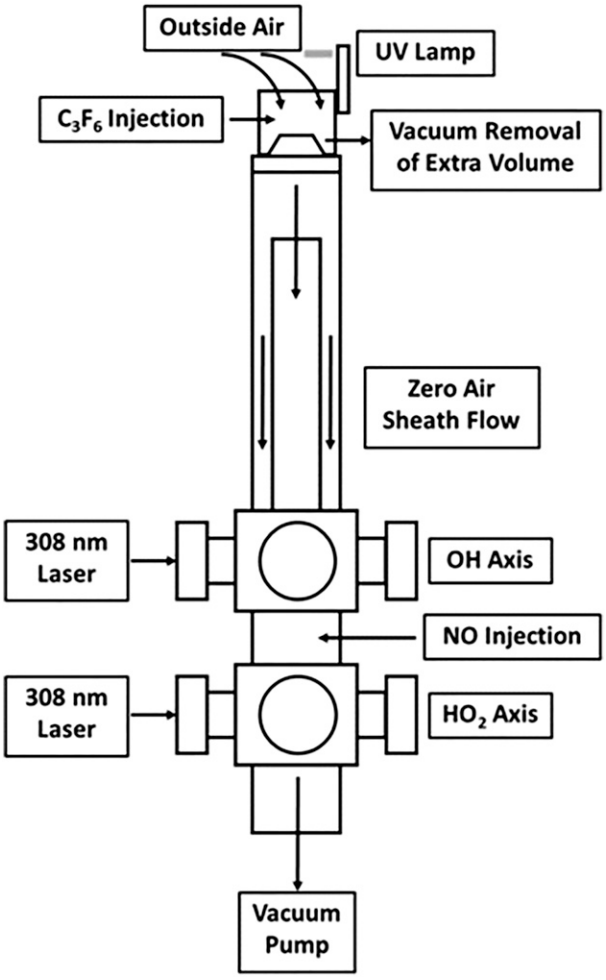

FIG. 1. Schematic diagram showing GTHOS as it was configured for SOAS. C_3F_6 was injected through six 0.25-mm needles that were pointed toward the center of the inlet. Attached just above and to the side of the inlet was a mercury lamp used for daily testing of the C_3F_6 injection system's effectiveness.

instrument. By turning C_3F_6 injection on and off, the ambient OH signal is determined by subtracting the signal when injection is on from the signal when injection is off. This method is called OH_{chem}. The difference between OH_{wave} and OH_{chem} is OH produced in the inlet or instrument, called OH_{int}. Tests for SOAS show that OH_{int} is not produced by the laser but rather by unknown chemistry occurring inside the instrument. To test the functionality of the OH scavenging system, a UV lamp was affixed to the instrument near the inlet. The lamp, which photolyzed water vapor to make a large abundance of ambient OH, was turned on for a few minutes three times a day to ensure that the C_3F_6 injection was scavenging OH properly. The absolute uncertainty of the OH_{chem} and OH_{int} measurements is $\pm 20\%$ (1σ confidence).

In addition to OH and HO_2 measurements, the OH reactivity was also determined and its measurement is described in detail elsewhere (Kovacs and Brune 2001; Mao et al. 2009). Approximately 150 L min^{-1} of ambient air is drawn into the instrument and flows through the 7.5-cm-diameter flow tube. At the far end of the flow tube is a sampling inlet and OH measurement system nearly identical to the one used in the main GTHOS system. Before the airflow reaches the sampling inlet, it flows past a movable source of OH called the wand. Inside the wand, 5 L min^{-1} of moist nitrogen flows past a mercury lamp, which photolyzes the water vapor to produce OH and HO_2 that are added to the ambient flow. As the wand moves away from the sampling inlet, the OH has more time to react with trace gases in the ambient air flowing through the tube and the OH signal decreases exponentially. Moving 10 cm is equivalent to a reaction time of 200 ms and the wand completes a cycle in 30 s. The OH reactivity is the slope of the logarithm of the OH signal divided by the reaction time.

The large suite of other measurements included meteorological parameters, inorganic species, VOCs, oxygenated VOCs (OVOCs), and many aerosol abundances and properties (NOAA 2016). There were also other measurements of OH by selective ion chemical ionization mass spectrometry (SICISM) and OH reactivity by the comparative reactivity method (CRM); these compare reasonably well with the ones reported here and are discussed in a separate manuscript (D. Sanchez et al. 2016, in preparation). Data used in this study were drawn primarily from measurements taken on the SOAS tower, though a few measurements that were unavailable or unreliable on the SOAS tower were instead taken from the SOAS trailers a few hundred yards away.

c. *Photochemical box modeling*

The HO_x measurements were compared to results from a photochemical box model (Wolfe and Thornton 2011) using two different chemical mechanisms, the Master Chemical Mechanism, version 3.2 (MCMv3.2) (Jenkin et al. 1997), augmented with explicit isoprene chemistry (Mao et al. 2012), and MCMv3.3.1 (Jenkin et al. 2015). These mechanisms have over 6700 unique chemical species that take part in roughly 17 000 different reactions. MCMv3.3.1 is an updated version of MCMv3.2 that contains an isoprene mechanism and did not need to be augmented. The difference between these two isoprene mechanisms appears to be mainly in the isoprene RO_2 isomerization pathways and products, which result in more OH regeneration in MCMv3.3.1 than in the augmented MCMv3.2. We report the results from augmented MCMv3.2 because it was used in BEARPEX, thus tying the modeling for the two forests

together. However, we focus our analysis on results from MCMv3.3.1.

The models were run so that model output was obtained at 10-min intervals for the entire SOAS campaign. The simultaneous measurements of other chemical species and of meteorological conditions were used to constrain the model with as many of the inputs as possible, except for OH and HO_2, which were being calculated (Table S1). Any data that were missing or otherwise unsuitable for integration into the model were removed and an interpolation was used to fill in for these missing data. Starting on 4 July (day of the year 185), 11 oxygenated species were no longer measured, including some acids and peroxides. The values for these chemical species were approximated for the model runs by finding other species that correlated strongly with them and then using these correlations to estimate the diel (24 h) variations of these chemical species. No significant changes in model performance or agreement between measured and modeled HO_x were observed after 4 July. To prevent the buildup of unmeasured oxygenated species in the model, a deposition rate of 1 day was assumed, although deposition rates from 12 h to 2 days gave nearly identical results for OH, HO_2, and OH reactivity. The data were averaged into 10-min time intervals for the modeling and the comparisons to measurements.

Photolysis frequencies (J values) were not measured during SOAS, so J values were calculated using the NCAR Tropospheric Ultraviolet and Visible Radiation Model (TUV) (Madronich and Weller 1990). TUV calculations assume clear overhead skies but use measured overhead ozone column, atmospheric scattering, and surface albedo. To account for the effects of overhead cloud cover, a method of determining $J\mathrm{NO_2}$ based on measurements of solar irradiance was used. By comparing these estimated values of $J\mathrm{NO_2}$ to those calculated by TUV, a correction factor was created and it varied between 30% and 80% of the clear-sky J values. This correction factor was then applied to the other photolysis frequencies calculated by TUV.

This method, described by Trebs et al. (2009), has been shown to produce accurate values for $J\mathrm{NO_2}$, but typically less accurate results for the photolysis frequency for $O_3 + h\nu \rightarrow O_2 + O(^1D)$, where $h\nu$ indicates solar ultraviolet radiation. During the recent SHARP study in Houston, Texas, in 2009, photolysis frequencies were measured (Ren et al. 2013) and $JO(^1D)$ calculated by this method was consistently lower than measured $JO(^1D)$ by 23%. Because the meteorological and cloud conditions during SHARP were similar to those during SOAS, this difference in $JO(^1D)$ suggests a similar uncertainty in the SOAS $JO(^1D)$ values. Using the higher $JO(^1D)$ values in MMv3.3.1 increased modeled OH by 10% and modeled HO_2 by 6%; thus, this uncertainty in the calculated photolysis frequencies must be considered as part of the model uncertainty.

d. *Measured and modeled HO_x comparison*

The results presented in this paper cover the period between 26 June and 14 July 2013. This period was selected because it had the greatest number of simultaneously measured chemical species that were used to constrain the model and the longest runs of continuous GTHOS data. These models and approximations have been used successfully before in other field studies (Mao et al. 2012; Ren et al. 2013). To assess the model uncertainty, we assume that a global uncertainty and sensitivity analysis from a previous related study using the RACM2 model (Chen et al. 2012) provides an estimate of the model uncertainty for SOAS. The estimated uncertainty (1σ confidence) is approximately $\pm 20\%$ for modeled OH and HO_2. However, because of the additional uncertainty in $JO(^1D)$, the estimated model uncertainty (1σ confidence) is increased to $\pm 25\%$. These uncertainty estimates are consistent with uncertainties derived for other models in low-NO_x conditions (Pilling 2008) and can be used to provide guidance for understanding the significance of the comparisons between the measured and modeled OH, HO_2, and OH reactivity in this study.

e. *RO_2 interference in HO_2 measurements*

Recently it has been shown that some alkylperoxy radicals from alkene and aromatic compounds (RO_2) can be an interference in HO_2 measurements that use nitric oxide (NO) to convert HO_2 to OH for detection (Fuchs et al. 2011). Similar to the HO_2 radicals, RO_2 radicals can be converted to OH through reactions with NO followed by rapid O_2 extraction of a hydrogen atom to form HO_2, which is then converted by NO to OH. This conversion from RO_2 to OH happens almost as quickly as the HO_2 to OH reaction, leading to an increase in measured HO_2 signal. This RO_2 interference has been quantified for several LIF instruments (Fuchs et al. 2011; Whalley et al. 2013) as well as for GTHOS (P. A. Feiner et al. 2016, in preparation). These studies show that a successful strategy to reduce this interference is to shorten the time between NO injection and OH detection and to add only enough NO to convert a small fraction of HO_2 to OH. In GTHOS, the reaction time was shortened to 3 ± 1 ms and the NO concentration for the HO_2 measurement was reduced to 1.2×10^{13} cm^{-3}. From laboratory and field measurements, the HO_2 conversion efficiency was 0.24 ± 0.03 and the relative conversion efficiency of isoprene compared to HO_2 was

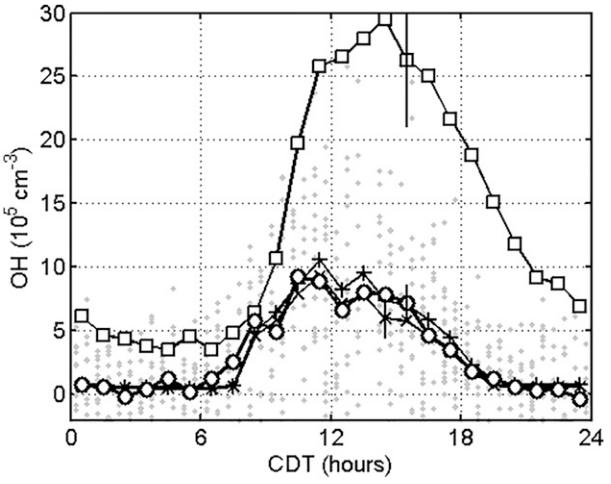

FIG. 2. Diel variation of OH_{chem} (○), OH_{int} (□), MCMv3.2 OH (×), and MCMv3.3.1 (+) for 26 Jun–14 Jul. Gray dots are individual 10-min measurements. OH is given in units of 10^5 cm^{-3}. The hours are in central daylight time. Error bars are ±20% for measured OH and ±25% for modeled OH, all at 1σ confidence levels.

6% ± 6%. This strategy increases the absolute uncertainty of the GTHOS HO_2 measurement from ±16% to ±20% (1σ confidence level) but it suppresses the interference.

3. Results

Two primary tests of the oxidation chemistry at SOAS are applied in this paper: 1) a comparison of measured and modeled OH and HO_2 as a function of different variables and 2) a budget analysis of OH production and loss. OH modeled with two different model mechanisms is compared to both OH_{chem}, which is demonstrated to be ambient OH, and OH_{int}, which is an interference signal. All of the following results come from the analysis of the 19-day period between 26 June and 14 July. The time series for JNO_2, OH, HO_2, NO, isoprene, and temperature are shown in Fig. S1. The entire dataset is available at a URL given in the online supplement.

a. *Comparisons of measured and modeled OH and HO_2*

Measured OH_{chem}, OH_{int}, and OH calculated by the model mechanisms were averaged into 1-h intervals to create median profiles (Fig. 2) for the 19-day period of measurements. The peak median daytime OH_{chem} was less than 10^6 OH cm^{-3}, although on some individual days it was twice as large. Median OH_{int} was as much as 3 times larger than OH_{chem} during daylight hours and, at night, median OH_{int} was about 5×10^5 cm^{-3} while median OH_{chem} was less than $\sim 2 \times 10^5$ cm^{-3}. OH_{int} behaved differently from OH_{chem}, peaking later in the day and persisting longer into the evening hours than OH_{chem} did. While the identity of OH_{int} is still unknown, this behavior suggests that OH_{int} results from chemistry involving long-lived oxygenated species and/or ozone, which can persist into the evening.

OH_{chem} agrees with OH calculated by both MCM chemical mechanisms over the entire diel cycle to well within combined measurement and model uncertainties. OH_{int} is more than double OH_{chem} and the models and extends well into the evening. The peak median measured daytime [OH] was 2–5 times larger than the GTHOS limit of detection for a 1-h average, which is estimated to be $\sim 2 \times 10^5$ to 3×10^5 cm^{-3}. When the 1-h averages for OH_{chem} are compared to OH calculated with augmented MCMv3.2, the linear least squares fit of OH_{chem} as a function of augmented MCMv3.2 OH gives a slope of 0.94 and an intercept of 4×10^4 cm^{-3}, with a coefficient of determination R^2 of 0.50 (Fig. S2). With MCMv3.3.1, the slope is 0.86 and the intercept is 2×10^4 cm^{-3}, with an R^2 of 0.52 (Fig. S3). OH calculated by MCMv3.3.1 is greater than that calculated by augmented MCMv3.2 because the MCMv3.3.1 mechanism regenerates more OH than the augmented MCMv3.2 does. Nevertheless, the two chemical mechanisms are consistent with the observed OH to well within uncertainties.

These results are similar to those found by Mao et al. (2012) and Hens et al. (2014), which is interesting because the forests in those studies were dominated by MBO chemistry with some distant isoprene influence and by terpene chemistry, respectively, while the SOAS forest was dominated by isoprene chemistry. Thus, OH_{int} cannot result from a particular chemical system but instead must come from a class of chemical species or reactions that are common to different forest chemistries.

Measured HO_2 and HO_2 calculated by the model mechanisms were averaged into 1-h intervals to create mean profiles (Fig. 3) for the 19-day period of measurements. The peak median daytime value for measured HO_2 was 27 pptv, although it was as high as 40 ppbv on a few hot, sunny days and as low as 8 pptv on a few cool, cloudy days (Fig. S1). The minimum median HO_2 was 2 pptv, which occurred in the morning at 0600 central daylight time (CDT). In the morning, HO_2 rises at the same time that the photolysis of formaldehyde (HCHO) rises, but after the peak value, the evening decay of HO_2 is much slower than the decrease in the HCHO photolysis.

The behavior of measured HO_2 matches that calculated by augmented MCMv3.2 and MCMv3.3.1, although the observed nighttime decay of HO_2 is much

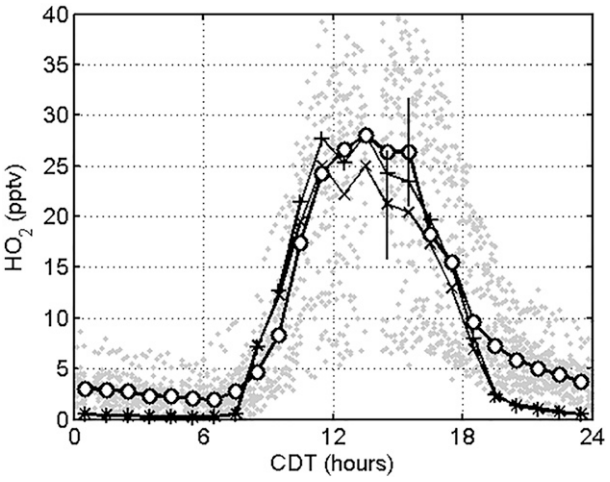

FIG. 3. Diel variation of measured HO_2 (○), MCMv3.2 HO_2 (×), and MCMv3.3.1 (+) for 26 Jun–14 Jul. Gray dots are individual 30-s measurements. HO_2 is given in units of pptv. The hours are in central daylight time. Error bars are ±20% for measured HO_2 and ±25% for modeled HO_2, all at 1σ confidence levels.

slower than the decay of modeled HO_2. The linear least squares fit of measured HO_2 as a function of augmented MCMv3.2 HO_2 gives a slope of 0.95 and an intercept of 2.6 pptv, with an R^2 of 0.82 (Fig. S2). For MCMv3.3.1, the slope is 0.84 and the intercept is 2.6 pptv, with an R^2 of 0.84 (Fig. S1). This agreement is well within the combined 1σ uncertainties of the measured and modeled HO_2.

When measured and modeled daytime OH are plotted against variables other than time of day, OH_{chem} has the same behavior as OH calculated by augmented MCMv3.2 and MCMv3.3.1 as a function of $JO(^1D)$, NO up to 0.8 pptv, and O_3 up to 60 ppbv (Fig. 4). Daytime is defined as the hours between 0700 and 1700 CDT. The behavior of measured and modeled OH agree for isoprene up to 7 ppbv, but above that amount, OH_{chem} diverges to become on average of $1.5 \times 10^6\,cm^{-3}$, about twice the modeled OH when isoprene was 11 ppbv, although this conclusion is based on only a few data points. The agreement between measured and modeled OH as a function of these four controlling variables is substantial.

In all cases except one, OH_{int} shows the same behavior as OH_{chem} as a function of other variables, except it has a greater magnitude and slope (Fig. 4). However, when plotted against NO, OH_{int} decreases from being 6 times larger than OH_{chem} at NO = 0.02 ppbv to being equal at NO = 0.3 ppbv, while OH_{chem} and the modeled OH decrease less than a factor of 2 over this same NO range. This decreasing interference signal with NO suggests that a low-NO oxidation pathway and the chemical species it generates are responsible for OH_{int} or that NO removes the chemical species responsible for OH_{int}.

When median measured and modeled daytime HO_2 are plotted against variables other than time of day, measured HO_2 has the same behavior as modeled HO_2 for $JO(^1D)$, NO, O_3, and isoprene (Fig. 4). However, measured HO_2 decreases faster than modeled HO_2 with increasing NO and increases slightly faster than modeled HO_2 with increasing O_3 and Isoprene. For NO above 0.1 pptv, measured HO_2 is only half HO_2 modeled with both augmented MCMv3.2 and MCM3.3.1. These higher NO values occur only in the morning between 0600 and 0900 CDT when HO_2 is rising rapidly as HO_x photolytic production begins, so small errors in the timing or values of the photolysis frequencies used in the model could explain this difference. All in all, the agreement between measured and modeled HO_2 as a function of these four controlling variables is generally within measurement and model uncertainties.

The SOAS results are different from those found by Mao et al. (2012) and Hens et al. (2014). In the California forest, HO_2 was not measured in a way that discriminated against the RO_2 interference, and so the measurement is more appropriately called HO_2^*, which is HO_2 and any RO_2 that are also converted by the addition of reagent NO. But even with this interference, measured HO_2 was less than modeled. In the Finland forest, HO_2 was measured in a way that discriminated against the RO_2 interference but it was 3.3 times the modeled HO_2. It is possible that these differences are caused by the differences in the dominant BVOC chemistry in these different forests, but this cause of the differences seems unlikely since measured and modeled OH are in good agreement in all three studies. Thus, the cause of these differences is unknown. Put in the context of these other studies, the agreement between measured and modeled HO_2 for SOAS is quite good.

b. *Measured OH reactivity*

The median measured OH reactivity reached a maximum of $26\,s^{-1}$ just after noon but remained above $22\,s^{-1}$ until 1800 CDT (Fig. 5). The median minimum was $11\,s^{-1}$ at 0400 CDT. Individual 30-s values ranged from 3 to $40\,s^{-1}$. A second OH reactivity measurement using the competitive reactivity method during SOAS gave values that track our OH reactivity values during the morning but were about 25% lower in the afternoon and evening (D. Sanchez et al. 2016, in preparation). The diel behavior of the measured OH reactivity is different from that in some other forests (Mao et al. 2009; Nölscher et al. 2012; Mogensen et al. 2011) and similar to that in others (Di Carlo et al. 2004; Griffith et al. 2016). Differences in OH reactivity behavior are driven by differences in the types of biogenic emissions,

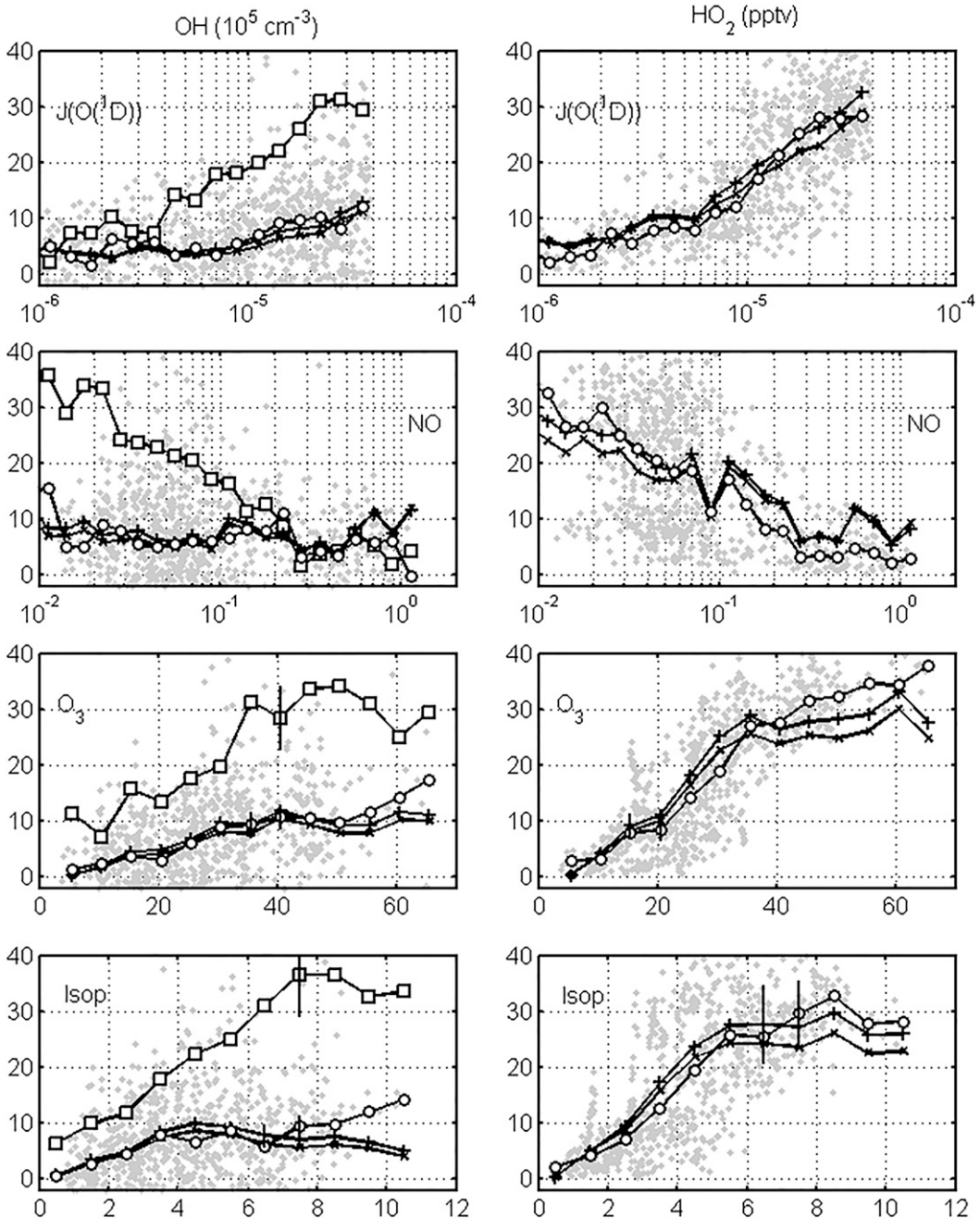

FIG. 4. (left) OH (10^5 cm^{-3}) and (right) HO_2 (pptv) as a function of (top)–(bottom) $JO(^1D)$ (s^{-1}), NO (ppbv), O_3 (ppbv), and isoprene (ppbv). Shown are median OH from measurements (○), augmented MCMv3.2 (×), and MCMv3.3.1 (+) and from the interference (□) and median HO_2 from measurements (○), augmented MCMv3.2 (×), and MCMv3.3.1 (+). Gray dots are individual measured data points. Uncertainties (black bars) are shown for the 1σ confidence level.

temperature, local topography, meteorology, and changing depth of the mixed layer.

A detailed analysis of the OH reactivity budget is provided by Kaiser et al. (2016). The median diel variation presented here is slightly different from that presented by Kaiser et al. because slightly different days are included in the median values. In that paper, they show that inorganic chemical species, isoprene, and its oxygenated products account for 90% of the OH reactivity at SOAS during the afternoon and about 80% at

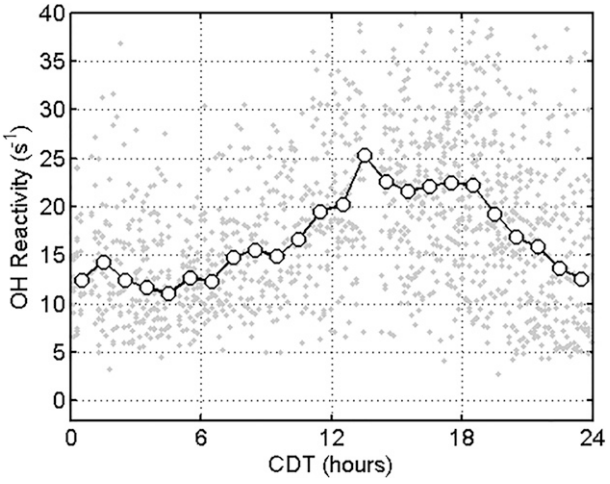

FIG. 5. Measured OH reactivity (s^{-1}). Diel variation is shown for measured OH reactivity (black circle and line) and individual 30-s measurements (gray dots).

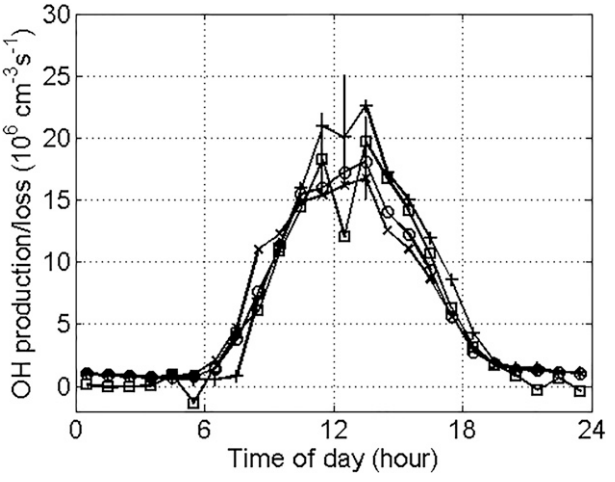

FIG. 6. Diel variation of OH production (○), OH loss (□), MCMv3.2 (×), and MCMv3.3.1 (+) OH production and loss, which are balanced. The absolute uncertainty for OH production and loss are 25% at 1σ confidence.

night. Isoprene alone accounts for about 60% of the measured OH reactivity during the afternoon. When the uncertainties in the measurements and model are taken into account, the 10%–20% difference between measured and modeled OH reactivities is within uncertainties for the daytime. Kaiser et al. provide evidence that any actual difference between measured and modeled OH reactivity would come from unmeasured primary emissions and not oxygenated isoprene products.

c. *OH budget analysis*

Given the OH reactivity of 10–30 s^{-1} (OH lifetime 33–100 ms), OH is in steady state for all times longer than 1 s and therefore OH production and loss rates are in balance. The OH loss rate is the product of the OH concentration and the OH reactivity—both of which are measured. Many of the contributions to the OH production rate consist of measured quantities, including a large contribution from HO_2 + NO, so the balance of OH production and loss using as many measured quantities as possible is a good test of the oxidation chemistry and the measurements.

Measured OH loss, OH production with measured chemical species, and MCMv3.2 and MCMv3.3.1 balanced OH production and loss were averaged into 1-h intervals to create median profiles for the 19-day period of measurements (Fig. 6). Median measured OH production and OH loss peaked between 1.8×10^7 and 2.0×10^7 $cm^{-3}s^{-1}$. The peak modeled OH production and loss is 2.2×10^7 $cm^{-3}s^{-1}$ for MCMv3.3.1 and 1.7×10^7 $cm^{-3}s^{-1}$ for augmented MCMv3.2, but both are within their overlapping uncertainties of each other. Thus the measured OH production and loss agree to well within 1σ uncertainty and they both also agree with OH production and loss calculated by both models to within their 1σ uncertainties.

The modeled OH production consists of three main terms: recycling from HO_2, primary photolysis of O_3 followed by the reaction of $O(^1D)$ and water vapor, and reaction sequences initiated by ozone. These reactions sequences initiated by ozone accounted for more than 80% of the OH production at night and about 20% during the day. HO_2 recycling by reaction with NO peaked at ~90% of the total production when NO was 0.23–0.3 ppbv between 0800 and 1000 CDT and was ~30% for the rest of the day. Primary production from $O(^1D)$ and water vapor accounted for 40%–50% of OH production between 1100 and 1700 CDT. Photolysis of the isoprene hydroperoxy aldehydes (HPALDs) from RO_2 isomerization chemistry accounted for at most a few percent of the OH production. Taken together, these terms accounted for more than 90% of the OH production over the entire diel cycle.

4. Discussion and conclusions

The Southern Oxidant and Aerosol Study has proven to be an excellent test of the updated isoprene chemical mechanisms. The OH measurement using chemical scavenging agrees with the modeled OH to well within combined 1σ uncertainties, while the interference measurement using LIF wavelength modulation is 3 times larger than the measured OH. And, unlike previous field studies in which measured and modeled OH agreed but measured and modeled HO_2 did not, the

measured and modeled HO_2 at SOAS also agree to within uncertainties. Finally, the measured OH loss rate and OH production rate calculated from measurements balance to well within measurement uncertainties, providing strong evidence that there was no large missing OH source at SOAS.

SOAS is the third study to demonstrate the critical importance of using the chemical removal method to measure OH. Even if some LIF-FAGE instruments appear to be free of interferences in the laboratory, they need to be outfitted with chemical removal systems to confirm the accuracy of atmospheric OH measurements made by the wavelength modulation technique. Further, it might be possible to develop an instrument that measures OH without pulling the sampled air through a pinhole inlet into a low-pressure detection region, which is presumably the source of the GTHOS interference signal. However, any new OH-measuring instrument will add little value to the understanding of forest atmospheric oxidation chemistry unless it can detect OH at levels close to $10^5\,cm^{-3}$.

There is now the question ''How extensive is this interference?'' If it extends beyond forests to urban areas, the upper boundary layer, the free troposphere, and into the stratosphere, then two decades of OH measurements could be affected. However, evidence from the laboratory and from field studies suggest that the interference is significant only in forests where the OH abundances are low but may have affected OH measurements by as much as 20%–30% in urban areas where the OH abundances are generally high (Ren et al. 2008, 2012; Brune et al. 2016). Studies are now beginning to test the hypothesis that this interference is significant only in forests.

The SOAS dataset is rich and it will take some time to adequately mine it. These results will need to be considered in the context of other measurements that can constrain the levels of atmospheric oxidants and other measurements that test more aspects of isoprene oxidation chemistry than measurements of OH and HO_2 by themselves can. All in all, these SOAS results demonstrate that the current understanding of isoprene oxidation chemistry correctly determines OH and HO_2 abundances to as well as it can be determined at this time. This chemistry can be incorporated with confidence into global models for studies dependent on OH abundances.

Acknowledgments. We thank the SOAS campaign organizers and leadership (A. M. Carlton, A. Goldstein, J. Jimenez, R. W. Pinder, J. de Gouw, B. J. Turpin, and A. B. Guenther), NCAR EOL personnel, and our hosts in Brent, Alabama, especially Mayor Dennis Stripling, for a successful field campaign. We also thank B. Baier for performing some model simulations and S. Kim and H. Harder for helpful conversations. SOAS financing and support was given by NSF, the NCAR Earth Observing Laboratory, and the Electric Power Research Institute. The Penn State effort was supported by NSF Grant AGS-1246918. Caltech acknowledges funding from the National Science Foundation (NSF) under Grant AGS-1240604 and NSF Postdoctoral Research Fellowship Program Award AGS-1331360. The University of Wisconsin–Madison and Harvard acknowledge funding from the National Science Foundation (NSF) under Grants AGS-1247421 and AGS-1628530.

REFERENCES

Brune, W. H., and Coauthors, 2016: Ozone production chemistry in the presence of urban plumes. *Faraday Discuss.*, **189**, 169–189, doi:10.1039/C5FD00204D.

Cantrell, C. A., G. D. Edwards, S. Stephens, L. Mauldin, E. Kosciuch, and M. Zondlo, 2003: Peroxy radical observations using chemical ionization, mass spectrometry during TOPSE. *J. Geophys. Res.*, **108**, 8371, doi:10.1029/2002JD002715.

Carlton, A. G., and Coauthors, 2016: The Southeast Atmosphere Studies (SAS): Coordinated investigation and discovery to answer critical questions about fundamental atmospheric processes. *Bull. Amer. Meteor. Soc.*, submitted.

Carslaw, N., and Coauthors, 2001: OH and HO_2 radical chemistry in a forested region of north-western Greece. *Atmos. Environ.*, **35**, 4725, doi:10.1016/S1352-2310(01)00089-9.

Chen, S., W. H. Brune, O. O. Oluwole, C. E. Kolb, F. Bacon, G. Y. Li, and H. Rabitz, 2012: Global sensitivity analysis of the regional atmospheric chemical mechanism: An application of random sampling-high dimensional model representation to urban oxidation chemistry. *Environ. Sci. Technol.*, **46**, 11 162–11 170, doi:10.1021/es301565w.

Crounse, J. D., F. Paulot, H. G. Kjaergaard, and P. O. Wennberg, 2011: Peroxy radical isomerization in the oxidation of isoprene. *Phys. Chem. Chem. Phys.*, **13**, 13 607–13 613, doi:10.1039/c1cp21330j.

——, H. C. Knap, K. B. Ørnsø, S. Jørgensen, F. Paulot, H. G. Kjaergaard, and P. O. Wennberg, 2012: On the atmospheric fate of methacrolein. 1. Peroxy radical isomerization following addition of OH and O_2. *J. Phys. Chem.*, **116A**, 5756–5762, doi:10.1021/jp211560u.

——, L. B. Nielsen, S. Jorgensen, H. G. Kjaergaard, and P. O. Wennberg, 2013: Autoxidation of organic compounds in the atmosphere. *J. Phys. Chem. Lett.*, **4**, 3513–3520, doi:10.1021/jz4019207.

Di Carlo, P., and Coauthors, 2004: Missing OH reactivity in a forest: Evidence for unknown reactive biogenic VOCs. *Science*, **304**, 722–725, doi:10.1126/science.1094392.

Faloona, I. C., and Coauthors, 2004: A laser-induced fluorescence instrument for detecting tropospheric OH and HO_2: Characteristics and calibration. *J. Atmos. Chem.*, **47**, 139–167, doi:10.1023/B:JOCH.0000021036.53185.0e.

Fuchs, H., B. Bohn, A. Hofzumahaus, F. Holland, K. Lu, S. Nehr, F. Rohrer, and A. Wahner, 2011: Detection of HO_2 by laser-induced fluorescence: Calibration and interferences from RO_2 radicals. *Atmos. Meas. Tech.*, **4**, 1209–1225, doi:10.5194/amt-4-1209-2011.

——, and Coauthors, 2013: Experimental evidence for efficient hydroxyl radical regeneration in isoprene oxidation. *Nat. Geosci.*, **6**, 1023–1026, doi:10.1038/ngeo1964.

Griffith, S. M., and Coauthors, 2016: Measurements of hydroxyl and hydroperoxy radicals during CalNex-LA: Model comparisons and radical budgets. *J. Geophys. Res. Atmos.*, **121**, 4211–4232, doi:10.1002/2015JD024358.

Hansen, D. A., E. S. Edgerton, B. E. Hartsell, J. J. Jansen, N. Kandasamy, G. M. Hidy, and C. L. Blanchard, 2003: The Southeastern Aerosol Research and Characterization Study: Part 1—Overview. J. *Air Waste Manage. Assoc.*, **53**, 1460–1471, doi:10.1080/10473289.2003.10466318.

Hens, K., and Coauthors, 2014: Observation and modelling of HO_x radicals in a boreal forest. *Atmos. Chem. Phys.*, **14**, 8723–8747, doi:10.5194/acp-14-8723-2014.

Hofzumahaus, A., and Coauthors, 2009: Amplified trace gas removal in the troposphere. *Science*, **324**, 1702–1704, doi:10.1126/science.1164566.

Jenkin, M. E., S. M. Saunders, and M. J. Pilling, 1997: The tropospheric degradation of volatile organic compounds: A protocol for mechanism development. *Atmos. Environ.*, **31**, 81–104, doi:10.1016/S1352-2310(96)00105-7.

——, J. C. Young, and A. R. Richard, 2015: The MCMv3.3.1 degradation scheme for isoprene. *Atmos. Chem. Phys.*, **15**, 11 433–11 459, doi:10.5194/acp-15-11433-2015.

Kaiser, J., and Coauthors, 2016: Speciation of OH reactivity above the canopy of an isoprene-dominated forest. *Atmos. Chem. Phys.*, **16**, 9349–9359, doi:10.5194/acp-16-9349-2016.

Kim, S., and Coauthors, 2013: Evaluation of HO_x sources and cycling using measurement-constrained model calculations in a 2-methyl-3-butene-2-ol (MBO) and monoterpene (MT) dominated ecosystem. *Atmos. Chem. Phys.*, **13**, 2031–2044, doi:10.5194/acp-13-2031-2013.

Kovacs, T., and W. Brune, 2001: Total OH loss rate measurement. *J. Atmos. Chem.*, **39**, 105–122, doi:10.1023/A:1010614113786.

Kubistin, D., and Coauthors, 2010: Hydroxyl radicals in the tropical troposphere over the Suriname rainforest: Comparison of measurements with the box model MECCA. *Atmos. Chem. Phys.*, **10**, 9705–9728, doi:10.5194/acp-10-9705-2010.

Lelieveld, J., and Coauthors, 2008: Atmospheric oxidation capacity sustained by a tropical forest. *Nature*, **452**, 737–740, doi:10.1038/nature06870.

Levy, H. I. I., 1971: Normal atmosphere: Large radical and formaldehyde concentrations predicted. *Science*, **173**, 141–143, doi:10.1126/science.173.3992.141.

Lou, S., and Coauthors, 2010: Atmospheric OH reactivities in the Pearl River Delta—China in summer 2006: Measurement and model results. *Atmos. Chem. Phys.*, **10**, 11 243–11 260, doi:10.5194/acp-10-11243-2010.

Madronich, S., and G. Weller, 1990: Numerical integration errors in calculated tropospheric photodissociation rate coefficients. *J. Atmos. Chem.*, **10**, 289–300, doi:10.1007/BF00053864.

Mao, J., and Coauthors, 2009: Airborne measurement of OH reactivity during INTEX-B. *Atmos. Chem. Phys.*, **9**, 163–173, doi:10.5194/acp-9-163-2009.

——, and Coauthors, 2012: Insights into hydroxyl measurements and atmospheric oxidation in a California forest. *Atmos. Chem. Phys.*, **12**, 8009–8020, doi:10.5194/acp-12-8009-2012.

Martinez, M., and Coauthors, 2010: Hydroxyl radicals in the tropical troposphere over the Suriname rainforest: Airborne measurements. *Atmos. Chem. Phys.*, **10**, 3759–3773, doi:10.5194/acp-10-3759-2010.

McKeen, S. A., and Coauthors, 1997: Photochemical modeling of hydroxyl and its relationship to other species during the Tropospheric OH Photochemistry Experiment. *J. Geophys. Res.*, **102**, 6467–6493, doi:10.1029/96JD03322.

Monks, P. S., 2005: Gas-phase radical chemistry in the troposphere. *Chem. Soc. Rev.*, **34**, 376–395, doi:10.1039/b307982c.

Mogensen, D., and Coauthors, 2011: Modelling atmospheric OH-reactivity in a boreal forest ecosystem. *Atmos. Chem. Phys.*, **11**, 9709–9719, doi:10.5194/acp-11-9709-2011.

Nölscher, A. C., and Coauthors, 2012: Summertime total OH reactivity measurements from boreal forest during HUMPPA-COPEC 2010. *Atmos. Chem. Phys.*, **12**, 8257–8270, doi:10.5194/acp-12-8257-2012.

NOAA, 2016: SOAS Centreville data. NOAA/ESRL, accessed 26 September 2016. [Available online at http://esrl.noaa.gov/csd/groups/csd7/measurements/2013senex/Ground/DataDownload/.]

Paulot, F., J. D. Crounse, H. G. Kjaergaard, A. Kürten, J. M. St. Clair, J. H. Seinfeld, and P. O. Wennberg, 2009: Unexpected epoxide formation in the gas-phase photooxidation of isoprene. *Science*, **325**, 730–733, doi:10.1126/science.1172910.

Peeters, J., and J.-F. Müller, 2010: HOx radical regeneration in isoprene oxidation via peroxy radical isomerisations. II: Experimental evidence and global impact. *Phys. Chem. Chem. Phys.*, **12**, 14 227–14 235, 10.1039/c0cp00811g.

——, T. L. Nguyen, and L. Vereecken, 2009: HO_x radical regeneration in the oxidation of isoprene. *Phys. Chem. Chem. Phys.*, **11**, 5935–5939, doi:10.1039/b908511d.

——, J.-F. Müller, T. Strvrakou, and V. S. Nguyen, 2014: Hydroxyl radical recycling in isoprene oxidation driven by hydrogen bonding and hydrogen tunneling: The upgraded LIM1 mechanism. *J. Phys. Chem.*, **118A**, 8625–8643, doi:10.1021/jp5033146.

Pilling, M. J., 2008: Simulating atmospheric gas-phase chemistry: Uncertainties and mechanism reduction problems. *Simulation and Assessment of Chemical Processes*, I. Barnes and M. M. Kharytonov, Eds., Springer Science, 83–93.

Praske, E., J. D. Crounse, K. H. Bates, T. Kurten, H. G. Kjaergaard, and P. O. Wennberg, 2015: Atmospheric fate of methyl vinyl ketone: Peroxy radical reactions with NO and HO_2. *J. Phys. Chem.*, **119A**, 4562–4572, doi:10.1021/jp5107058.

Pugh, T. A. M., and Coauthors, 2010: Simulating atmospheric composition over a South-East Asian tropical rainforest: Performance of a chemistry box model. *Atmos. Chem. Phys.*, **10**, 279–298, doi:10.5194/acp-10-279-2010.

Ren, X., and Coauthors, 2006: OH, HO_2, and OH reactivity during the PMTACS–NY Whiteface Mountain 2002 campaign: Observations and model comparison. *J. Geophys. Res.*, **111**, D10S03, doi:10.1029/2005JD006126.

——, and Coauthors, 2008: HO_x chemistry during INTEX-A 2004: Observation, model calculation, and comparison with previous studies. *J. Geophys. Res.*, **113**, D05310, doi:10.1029/2007JD009166.

——, and Coauthors, 2012: Airborne intercomparison of HO_x measurements using laser-induced fluorescence and chemical ionization mass spectrometry during ARCTAS. *Atmos. Meas. Tech.*, **5**, 2025–2037, doi:10.5194/amt-5-2025-2012.

——, and Coauthors, 2013: Atmospheric oxidation chemistry and ozone production: Results from SHARP 2009 in Houston, Texas. *J. Geophys. Res. Atmos.*, **118**, 5770–5780, doi:10.1002/jgrd.50342.

Rohrer, F., and Coauthors, 2014: Maximum efficiency in the hydroxyl-radical-based self-cleansing of the troposphere. *Nat. Geosci.*, **7**, 559–563, doi:10.1038/ngeo2199.

St. Clair, J. M., and Coauthors, 2015: Kinetics and products of the reaction of the first-generation isoprene hydroxy hydroperoxide

(ISOPOOH) with OH. *J. Phys. Chem.*, **120A**, 1441–1451, doi:10.1021/acs.jpca.5b06532.

Stone, D., and Coauthors, 2011: Isoprene oxidation mechanisms: Measurements and modelling of OH and HO_2 over a South-East Asian tropical rainforest during the OP3 field campaign. *Atmos. Chem. Phys.*, **11**, 6749–6771, doi:10.5194/acp-11-6749-2011.

——, L. K. Whalley, and D. E. Heard, 2012: Tropospheric OH and HO_2 radicals: Field measurements and model comparisons. *Chem. Soc. Rev.*, **41**, 6348–6404, doi:10.1039/c2cs35140d.

Tan, D., and Coauthors, 2001: HO_x budgets in a deciduous forest: Results from the PROPHET summer 1998 campaign. *J. Geophys. Res.*, **106**, 24 407–24 427, doi:10.1029/2001JD900016.

Taraborrelli, D., M. G. Lawrence, J. N. Crowley, T. J. Dillon, S. Gromov, C. B. M. Gros, L. Vereecken, and J. Lelieveld, 2012: Hydroxyl radical buffered by isoprene oxidation over tropical forests. *Nat. Geosci.*, **5**, 190–193, doi:10.1038/ngeo1405.

Trebs, I., and Coauthors, 2009: Relationship between the NO_2 photolysis frequency and the solar global irradiance. *Atmos. Meas. Tech.*, **2**, 725–739, doi:10.5194/amt-2-725-2009.

Wennberg, P. O., and Coauthors, 1994: Removal of stratospheric O_3 by radicals: In situ measurements of OH, HO_2, NO, NO_2, ClO, and BrO. *Science*, **266**, 398–404, doi:10.1126/science.266.5184.398.

Whalley, L. K., and Coauthors, 2011: Quantifying the magnitude of a missing hydroxyl radical source in a tropical rainforest. *Atmos. Chem. Phys.*, **11**, 7223–7233, doi:10.5194/acp-11-7223-2011.

——, M. A. Blitz, M. Desservettaz, P. W. Seakins, and D. E. Heard, 2013: Reporting the sensitivity of laser-induced fluorescence instruments used for HO_2 detection to an interference from RO_2 radicals and introducing a novel approach that enables HO_2 and certain RO_2 types to be selectively measured. *Atmos. Meas. Tech.*, **6**, 3425–3440, doi:10.5194/amt-6-3425-2013.

Wolfe, G. M., and J. A. Thornton, 2011: The Chemistry of Atmosphere-Forest Exchange (CAFE) Model—Part 1: Model description and characterization. *Atmos. Chem. Phys.*, **11**, 77–101, doi:10.5194/acp-11-77-2011.

——, ——, M. McKay, and A. H. Goldstein, 2011: Forest-atmosphere exchange of ozone: Sensitivity to very reactive biogenic VOC emissions and implications for in-canopy photochemistry. *Atmos. Chem. Phys.*, **11**, 7875–7891, doi:10.5194/acp-11-7875-2011.